Articles

Contribution from the Anorganisch Chemisch Laboratorium, J. H. van't Hoff Instituut, Universiteit van Amsterdam, Nieuwe Achtergracht 166, 1018 WV Amsterdam, The Netherlands

Spectroscopy and Photochemistry of Nickel(0)–α-Diimine Complexes. 1.[1] Structural Differences among NiL_2 and $Ni(CO)_2L$ (L = α-Diimine) Complexes: Molecular Orbital Calculations and an Electronic Absorption and Resonance Raman Study

Peter C. Servaas, Derk J. Stufkens,* and Ad Oskam

Received May 18, 1988

This article describes the MO diagrams and electronic absorption and resonance Raman (RR) spectra of a series of complexes of the types $Ni(R\text{-}DAB)_2$, $Ni(CO)_2(R\text{-}DAB)$, and $Ni(CO)_2(R\text{-}pyca)$ (DAB = 1,4-diaza-1,3-butadiene; pyca = pyridine-2-carbaldehyde imine). Major differences in the electronic and RR spectra of these complexes are attributed to differences in molecular structure (tetrahedral vs pseudoplanar) and rationalized with the use of MO diagrams derived from CNDO/s calculations on these complexes.

Introduction

All low-valence transition-metal α-diimine complexes possess an intense absorption band in the visible region that shows the characteristic features of a metal to α-diimine charge-transfer (MLCT) transition. The spectroscopic, photophysical, and photochemical properties of quite a few of these complexes have already been studied.[2-16] Resonance Raman (RR) spectroscopy appeared to be an especially valuable technique for the characterization of such allowed MLCT transitions.[17-28] Different electronic transitions within one single MLCT band could even be detected and identified with the use of RR excitation profiles.[29-36] The MLCT character of the transitions appeared to depend on the α-diimine ligand used. The transitions of the complexes of 2,2′-bipyridine (L = bpy) and 1,10-phenanthroline (L = phen) such as $Ru(L)_3^{2+}$, $Re(CO)_3LX$ (X = Cl, Br), $M(CO)_4L$ (M = Cr, Mo, W), and $Fe_2(CO)_7L$ all show a strong MLCT character. On the other hand, complexes of the α-diimine ligands R-DAB and R-pyca[37] are characterized by a much stronger interaction between one of the metal d_π orbitals and the lowest π^* orbital of the ligand (π back-bonding). As a result the strongly allowed electronic transition between these orbitals has much less MLCT character. This MLCT character can even completely disappear, as for example in the case of the $W(CO)_4(R\text{-}DAB)$[28] and $M(CO)_3(R\text{-}DAB)$ (M = Fe, Ru)[22,34] complexes. Such differences in MLCT character can generally not be deduced from the absorption spectra themselves but are clearly reflected in the RR spectra obtained by excitation into these transitions. RR spectra of complexes with a main electronic transition having considerable MLCT character show high intensities for symmetrical ligand stretching modes. When the main electronic transition has hardly any MLCT character but is instead metal–ligand bonding to antibonding, strong RR effects are observed for metal–ligand stretching and ligand deformation modes.[38]

RR spectroscopy becomes even more important when the allowed electronic transition is directly related to a reactive excited state. The observed photochemical processes can then be rationalized with the use of these RR data. Recently, this approach has been used successfully for the interpretation of the MLCT photochemistry of the complexes $Fe(CO)_3(R\text{-}DAB)$.[39] Normally, such low-valence α-diimine complexes with a lowest MLCT excited state are not very reactive since the weakening of the covalent metal–ligand bond is often compensated by a strengthening of the ionic interaction in this state. If they react anyway, this is normally caused by the presence of a close-lying, more reactive (e.g. LF) excited state.[40] Although the complexes $Ni(CO)_2(\alpha\text{-diimine})$ have no such reactive LF states ($3d^{10}$ configuration), preliminary measurements on these complexes indicated that they

* To whom correspondence should be addressed.

(1) Part 2: Servaas, P. C.; Stufkens, D. J.; Oskam, A. *Inorg. Chem.*, following paper in this issue.
(2) Wrighton, M. S.; Morse, D. L. *J. Am. Chem. Soc.* **1974**, *96*, 998.
(3) Kokkes, M. W.; Stufkens, D. J.; Oskam, A. *Inorg. Chem.* **1985**, *24*, 4411.
(4) Allen, G. H.; White, R. P.; Rillema, D. P.; Meyer, T. J. *J. Am. Chem. Soc.* **1984**, *106*, 2613.
(5) DeArmond, M. K.; Carlin, C. M. *Coord. Chem. Rev.* **1981**, *36*, 325.
(6) Kokkes, M. W.; Stufkens, D. J.; Oskam, A. *J. Organomet. Chem.* **1985**, *294*, 59.
(7) Caspar, J. V.; Westmoreland, T. D.; Allen, G. H.; Bradley, P. G.; Meyer, T. J.; Woodruff, W. H. *J. Am. Chem. Soc.* **1984**, *106*, 3492.
(8) Schadt, M. J.; Gresalfi, N. J.; Lees, A. J. *J. Chem. Soc., Chem. Commun.* **1984**, 507.
(9) Nishizawa, M.; Suzuki, T. M.; Sprouse, S.; Watts, R. J.; Ford, P. C. *Inorg. Chem.* **1984**, *23*, 1837.
(10) Kokkes, M. W.; Stufkens, D. J.; Oskam, A. *Inorg. Chem.* **1985**, *24*, 2934.
(11) Manuta, D. M.; Lees, A. J. *Inorg. Chem.* **1986**, *25*, 1354.
(12) Hill, R. H.; Puddephatt, R. J. *J. Am. Chem. Soc.* **1985**, *107*, 1218.
(13) Kober, E. M.; Meyer, T. J. *Inorg. Chem.* **1985**, *24*, 106.
(14) Phifer, C. C.; McMillin, D. R. *Inorg. Chem.* **1986**, *25*, 1329.
(15) Ichinaga, A. K.; Kirchhoff, J. R.; McMillin, D. R.; Dietrich-Buchecker, C. O.; Marnot, P. A.; Sauvage, J.-P. *Inorg. Chem.* **1987**, *26*, 4290.
(16) Van Dijk, H. K.; Stufkens, D. J.; Oskam, A.; Rotteveel, M.; Heijdenrijk, D. *Organometallics* **1987**, *6*, 1665.
(17) Dallinger, R. F.; Woodruff, W. H. *J. Am. Chem. Soc.* **1979**, *101*, 4391.
(18) Czernuszewicz, R. S.; Nakamoto, K.; Strommen, D. P. *Inorg. Chem.* **1980**, *19*, 793.
(19) Forster, M.; Hester, R. E. *Chem. Phys. Lett.* **1981**, *81*, 42.
(20) Balk, R. W.; Snoeck, T. L.; Stufkens, D. J.; Oskam, A. *Inorg. Chem.* **1980**, *19*, 3015.
(21) Balk, R. W.; Stufkens, D. J.; Oskam, A. *Inorg. Chim. Acta* **1981**, *48*, 105.
(22) Balk, R. W.; Stufkens, D. J.; Oskam, A. *J. Chem. Soc., Dalton Trans.* **1982**, 275.
(23) Bradley, P. G.; Kress, N.; Homberger, B. A.; Dallinger, R. F.; Woodruff, W. H. *J. Am. Chem. Soc.* **1981**, *103*, 7441.
(24) Basu, M.; Gafney, H. D.; Strekas, T. C. *Inorg. Chem.* **1982**, *21*, 2231.
(25) Smothers, W. K.; Wrighton, M. S. *J. Am. Chem. Soc.* **1983**, *105*, 1067.
(26) McClanahan, S.; Hayes, T.; Kincaid, J. *J. Am. Chem. Soc.* **1983**, *105*, 4486.
(27) Kokkes, M. W.; Snoeck, T. L.; Stufkens, D. J.; Oskam, A.; Cristophersen, M.; Stam, C. H. *J. Mol. Struct.* **1985**, *131*, 11.
(28) Van Dijk, H. K.; Servaas, P. C.; Stufkens, D. J.; Oskam, A. *Inorg. Chim. Acta* **1985**, *104*, 179.
(29) Streusand, B.; Kowal, A. T.; Strommen, D. P.; Nakamoto, J. *J. Inorg. Nucl. Chem.* **1977**, *39*, 1767.
(30) Clark, R. J. H.; Turtle, P. C.; Strommen, D. P.; Streusand, B.; Kincaid, J.; Nakamoto, K. *Inorg. Chem.* **1977**, *16*, 84.
(31) Balk, R. W.; Stufkens, D. J.; Oskam, A. *Inorg. Chim. Acta* **1978**, *28*, 133.

0020-1669/89/1328-1774$01.50/0

Table I. Bonding Parameters (β) and Electron Repulsion Parameters (γ) Used in the CNDO/s Calculations (eV)

β Values				
H	C	N	O	Ni
−13.6	−19.5	−25.5	−32.4	−9.39 (β_s) −4.77 (β_p) −17.57 (β_d)

γ Values					
γ_{ss}	γ_{sp}	γ_{sd}	γ_{pp}	γ_{pd}	γ_{dd}
9.648	9.648	9.957	8.300	9.957	16.556 (12.886)[a]

[a] Value used for Ni(H-DAB)$_2$ complexes.

do react photochemically. This means that the lowest ^{3}MLCT states of these complexes are reactive. In the case of the Ni(CO)$_2$(R-DAB) complexes different types of reactions could even be observed, depending on the substituent R.

In order to explain these observations, the electronic absorption and RR spectra of these complexes were studied in detail and related to the ground- and excited-state properties derived from MO calculations. These results are reported in this article, while the photochemical data of these complexes are discussed in a subsequent article.[1]

Although little is known, apart from two crystal structures,[41,42] about these Ni(CO)$_2$(α-diimine) complexes, other Ni(0) and Ni(II) complexes containing R-DAB ligands were extensively studied.[43-49] Different structures were found by tom Dieck and co-workers[46,47] for the complexes Ni(R-DAB)$_2$ depending on the R group at the coordinating nitrogen atoms of the R-DAB ligand. These structural differences were accompanied by typical changes in the electronic absorption and NMR spectra. In view of these results, the spectroscopic data of both types of complexes Ni(CO)$_2$(R-DAB) and Ni(R-DAB)$_2$ are reported here and discussed in relationship with each other.

Experimental Section

Preparations. All NiL$_2$ (L = 1,5-cyclooctadiene (COD), R-DAB) complexes were synthesized by literature procedures[46,47] and were carefully purified before use. All Ni(CO)$_2$(α-diimine) complexes were prepared according to the method described hereafter for Ni(CO)$_2$(tBu-DAB).

Ni(COD)$_2$(3 mmol) and tBu-DAB (3 mmol) were stirred for 1.5 h in 25 mL of *n*-hexane under a nitrogen atmosphere. After 15 min the solution turned purple due to the formation of Ni(COD)(tBu-DAB). After another 1.5 h a CO gas stream was thoroughly bubbled through for 7 min and the solution was stirred for 1 h under this CO atmosphere. Filtration of the solution was followed by recrystallization at −80 °C. Further purification was achieved by recrystallization from *n*-pentane and in the case of Ni(CO)$_2$(2,6-iPr$_2$Ph-DAB) by column chromatography, in the dark, on reversed-phase silica with pure *n*-pentane as the eluent.

Spectra. All spectroscopic samples were prepared by standard inert-gas techniques. The solvents used were of a spectroscopic grade, and they were distilled several times before use and carefully deoxygenated. The IR spectra were measured on a Nicolet 7199B FT-IR interferometer with a liquid-nitrogen-cooled Hg, Cd, Te detector (32 scans, resolution 0.5 cm^{-1}). A Perkin-Elmer Lambda 5 spectrophotometer was used to record the electronic absorption spectra. The resonance Raman (RR) spectra were recorded on a Jobin Yvon HG2S Ramanor instrument using an SP Model 171 Ar$^+$ laser and a CR 490 tunable dye laser with Coumarin 6, Rhodamine 6G, and Rhodamine 101 as dyes. An Anaspec 300-S filter with a band-pass of ~0.4 nm was used as a premonochromator. All RR spectra were recorded with a spinning cell, the windows of which are made of optical quality quartz. The spectra were corrected for decomposition in the laser beam. The ^{1}H NMR spectra were recorded on a Bruker AC100 NMR apparatus.

MO Calculations. CNDO/s calculations[50] have been performed on the model complexes Ni(H-DAB)$_2$ and Ni(CO)$_2$(H-DAB) with several dihedral angles. In these calculations standard CNDO/s parameters have been used for C, H, N, and O with the exception of the bonding parameter β. These values as well as those of β_s, β_p, and β_d for Ni are presented in Table I. Also included in this table are the values of the electron repulsion integrals γ. For Ni a basis set of Clementi double-ζ quality has been used.

The value of γ_{dd} used in the calculations of Ni(H-DAB)$_2$ differs from that normally applied by us in calculations of transition-metal carbonyls.[51] This is due to the fact that in a Ni d^{10} configuration the d orbitals are more diffuse, an effect that is not included in the γ_{dd} value normally used. In particular for the complexes Ni(H-DAB)$_2$ with a pseudoplanar geometry the strong repulsion between the Ni d_{yz} orbital and the nitrogen lone-pair orbitals can then result in an unrealistic destabilization of the Ni d_{yz} orbital which implies that the calculations lead to a d^8 configuration for these complexes. Therefore, a more realistic value of γ_{dd} has been calculated for Ni(H-DAB)$_2$:

$$\gamma_{dd} = 2\left(\left(\frac{\delta E_{el}}{\delta n_d}\right)_{s^0d^{10}} - \left(\frac{\delta E_{el}}{\delta n_d}\right)_{s^0d^{9.5}}\right) = 12.886 \text{ eV}$$

Usually one applies *I*–*A* to calculate γ_{dd}. This would, however, demand a Ni d^{11} configuration for the determination of *A*.

Table II. Infrared ν(CO) Frequencies of Ni(CO)$_2$(α-diimine) Complexes[a]

ligand	ν_s(CO), cm^{-1}	ν_{as}(CO), cm^{-1}
tBu-DAB	2004	1944
cHex-DAB[b]	2008	1945
iPr-DAB[b]	2006	1945
4-MePh-DAB[b]	2016	1966
2,6-Me$_2$Ph-DAB[b]	2023	1971
2,6-iPr$_2$Ph-DAB	2022	1970
2,4,6-Me$_3$Ph-DAB[b]	2021	1968
tBu-pyca	1994	1931
2,6-iPr$_2$Ph-pyca	1982	1924

[a] Measured in *n*-hexane. [b] Complexes made in situ according to ref 1.

Results and Discussion

The main route used for the preparation of Ni(CO)$_2$(α-diimine) complexes is

$$\underset{}{\text{Ni(COD)}_2} + \text{L} \rightarrow \underset{\text{I}}{\text{Ni(COD)L}} \xrightarrow{\text{CO}} \underset{\text{II}}{\text{Ni(CO)}_2\text{L}}$$

L = α-diimine

(32) Miller, P. J.; Chao, R. S.-L. *J. Raman Spectrosc.* **1979**, *8*, 17.
(33) Balk, R. W.; Stufkens, D. J.; Oskam, A. *Inorg. Chim. Acta* **1979**, *34*, 267.
(34) Kokkes, M. W.; Stufkens, D. J.; Oskam, A. *J. Chem. Soc., Dalton Trans* **1983**, 439.
(35) Griffiths, L.; Straughan, B. P.; Gardiner, D. J. *J. Chem. Soc., Dalton Trans.* **1983**, 305.
(36) Servaas, P. C.; van Dijk, H. K.; Snoeck, T. L.; Stufkens, D. J.; Oskam, A. *Inorg. Chem.* **1985**, *24*, 4494.
(37) The abbreviations DAB (1,4-diaza-1,3-butadiene) and pyca (pyridine-2-carbaldehyde imine) in this paper, used for economy of space, imply that the α-diimine carbon atoms are protonated (R-DAB, RN=CH—CH=NR; R-pyca, C$_5$H$_4$N—CH=NR). So, for R = *tert*-butyl = tBu, tBu—N=CH—CH=N—tBu becomes tBu—DAB (=tBu—DAB{H,H}). Other important abbreviations for the R groups used throughout this paper are Me = methyl, Ph = phenyl, iPr = isopropyl, and cHex = cyclohexyl (van Koten, G.; Vrieze, K. *Adv. Organomet. Chem.* **1982**, *21*, 151).
(38) Stufkens, D. J. *J. Mol. Struct.* **1982**, *79*, 67 and references therein.
(39) Van Dijk, H. K.; Stufkens, D. J.; Oskam, A. *J. Am. Chem. Soc.* **1989**, *111*, 541.
(40) Meyer, T. J. *Pure Appl. Chem.* **1986**, *58*, 1193 and references therein.
(41) Hausen, H. D.; Krogmann, K. *Z. Anorg. Allg. Chem.* **1972**, *389*, 247.
(42) Sieler, J.; Than, N. N.; Benedix, R.; Dinjus, E.; Walther, D. *Z. Anorg. Allg. Chem.* **1985**, *522*, 131.
(43) tom Dieck, H.; Lauer, A. M.; Stamp, L.; Diercks, R. *J. Mol. Catal.* **1986**, *35*, 317.
(44) Walther, D. *Z. Anorg. Allg. Chem.* **1977**, *431*, 17.
(45) Svoboda, M.; tom Dieck, H. *J. Organomet. Chem.* **1980**, *191*, 321.
(46) Svoboda, M.; tom Dieck, H.; Krüger, C.; Tsay, Y. H. *Z. Naturforsch.* **1981**, *36B*, 814.
(47) tom Dieck, H.; Svoboda, M.; Greiser, T. *Z. Naturforsch.* **1981**, *36B*, 823.
(48) Benedix, R.; Pitsch, D.; Schöne, K.; Hennig, H. *Z. Anorg. Allg. Chem.* **1986**, *542*, 102.
(49) Benedix, R.; Hennig, H. *Inorg. Chim. Acta* **1988**, *141*, 21.
(50) Del Bene, J.; Jaffé, H. H. *J. Chem. Phys.* **1968**, *48*, 1807.
(51) Andréa, R. R.; Louwen, J. N.; Kokkes, M. W.; Stufkens, D. J.; Oskam, A. *J. Organomet. Chem.* **1985**, *281*, 273.

Table III. Electronic Absorption Spectral Data of $Ni(CO)_2(\alpha$-diimine) and $Ni(R\text{-}DAB)_2$ Complexes[a]

complex	structure	λ_{max}, nm[b] (ϵ_{max}, M^{-1} cm^{-1})[d]	Δ_{max}, 10^3 cm^{-1} [c]
$Ni(CO)_2$(tBu-DAB)	tetrahedral	517	1.15
$Ni(CO)_2$(cHex-DAB)[e]	tetrahedral	508	
$Ni(CO)_2$(iPr-DAB)[e]	tetrahedral	508	
$Ni(CO)_2$(2,6-iPr_2Ph-DAB)	pseudoplanar	541	0.39
$Ni(CO)_2$(tBu-pyca)	tetrahedral	529	2.58
$Ni(CO)_2$(2,6-iPr_2Ph-pyca)	tetrahedral	557	2.23
$Ni(tBu\text{-}DAB)_2$	tetrahedral	475 (8000)	0
$Ni(cHex\text{-}DAB)_2$	tetrahedral	478 (9100)	0
$Ni(4\text{-}MePh\text{-}DAB)_2$	tetrahedral	529 (11 000)	0
$Ni(2,6\text{-}Me_2Ph\text{-}DAB)_2$	pseudoplanar	484 (8200), 738 (6600)	0

[a] Measured in benzene. [b] Maximum of the main MLCT transition(s). [c] $\Delta_{max} = \sigma_{max}(CH_3CN) - \sigma_{max}(C_6H_{12})$. [d] The ϵ_{max} values of the $Ni(CO)_2L$ complexes could not be determined reproducibly due to the high air sensitivity of these complexes. [e] Measured in situ according to ref 1.

In the case of L = R-DAB this method meets, however, with two main problems. First of all, complex I can react rapidly with R-DAB to give $Ni(R\text{-}DAB)_2$ (III), particularly when R is not a bulky aliphatic or aromatic group. This side reaction only occurs for α-diimine ligands with a strong π-acceptor capacity (R-DAB) and not for ligands such as bipyridine. For the latter ligand even the crystal structure of Ni(COD)(bpy) could be determined.[52]

Second, most of the $Ni(CO)_2$(R-DAB) complexes are rather air-sensitive and unstable in solution, which makes it very difficult to separate product mixtures of I, II, and III properly. As a result only those $Ni(CO)_2$(R-DAB) complexes could be prepared that have bulky substituents R at the coordinating nitrogen atoms. Also, two $Ni(CO)_2$(R-pyca) complexes have been prepared in a similar way. The instability of all these complexes implied that they had to be handled very carefully under nitrogen.

The IR spectra of the complexes II show two intense bands in the carbonyl stretching region belonging to $\nu_s(CO)$ and $\nu_{as}(CO)$. The frequencies of these bands are presented in Table II for several of these complexes, some of which have been made in situ.[1]

General trends with respect to the π-acceptor capacities of the α-diimine ligands are evident from this table. R-DAB is more π-accepting than R-pyca, and ligands with aromatic R groups are the strongest π-acceptors. Only very weak IR bands are observed in the CN stretching region for both complexes II and III in agreement with the results of Svoboda et al.[46] for these complexes and with the data of $Fe(R\text{-}DAB)_2$.[53]

Electronic Absorption Spectra. All complexes under study show one or more intense absorption bands in the visible region. Ni is formally zero valent in these complexes, which means that all Ni 3d orbitals are occupied and no LF transitions will occur. The absorption spectra will only contain MLCT and intraligand (IL) transitions.

Table III shows the main electronic absorption data of both the $Ni(R\text{-}DAB)_2$ and the $Ni(CO)_2(\alpha$-diimine) complexes.

(i) $Ni(R\text{-}DAB)_2$. tom Dieck and co-workers studied the absorption spectra of several $Ni(R\text{-}DAB)_2$ complexes, the structures of which varied from tetrahedral to pseudoplanar.[46,47] Both types of complexes possess an intense absorption band between 450 and 550 nm, whereas the pseudoplanar ones show an extra band between 700 and 800 nm. The authors did not assign these bands, nor did they explain the appearance of the low-energy band in the case of the pseudoplanar complexes.

MO calculations following the CNDO/s method of both the tetrahedral and the pseudoplanar type $Ni(R\text{-}DAB)_2$ complexes have been performed, with use of known bond distances and angles of the structures obtained in the literature.[46,47] The relevant parts of the MO schemes are shown in Figure 1 together with the

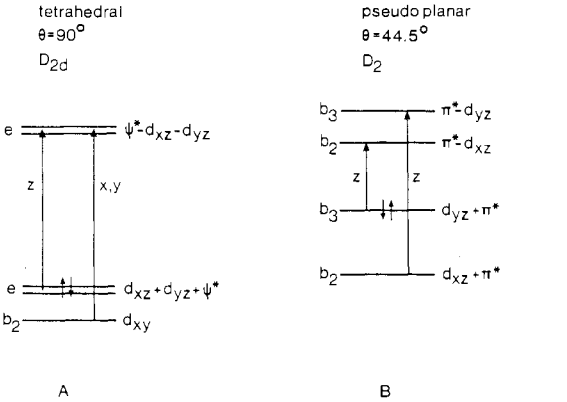

Figure 1. Relevant parts of the MO diagrams, including the electronic transitions with their polarization directions, of $Ni(R\text{-}DAB)_2$ complexes with tetrahedral (A) and pseudoplanar (B) structures.

symmetry-allowed MLCT transitions.

For the tetrahedral compounds the highest occupied orbital is the doubly degenerate e level with predominant metal d_{xz} and d_{yz} character (the z axis is the S_4 axis in this D_{2d} system). The LUMO is also doubly degenerate (e symmetry), which consists mainly of linear combinations of the π^* orbitals of the two R-DAB ligands, labeled as ψ^* by the designation of Orgel.[54] Four $e(d_{xz} + d_{yz} + \psi^*) \rightarrow e(\psi^* - d_{xz} - d_{yz})$ transitions are possible,[63] giving rise to four excited states with A_1, A_2, B_1, and B_2 symmetry, respectively. From these transitions only the one resulting in a B_2 excited state is expected to be intense. The reason is that the direction of charge transfer during this transition is parallel to the induced electric dipole, which is the z axis of the molecule. Transitions from the three lower lying d orbitals to the $e(\psi^* - d_{xz} - d_{yz})$ orbital are all polarized in the xy plane and therefore expected to be less intense. These latter transitions are situated at the high-energy side of the absorption band in the visible region. These data and assignments, which are in good agreement with those obtained for the isoelectronic d^{10} $Cu(R\text{-}DAB)_2^+$ complexes,[53,54] will be further corroborated by the RR spectra (vide infra).

A qualitative MO diagram of a pseudoplanar $Ni(R\text{-}DAB)_2$ complex with a dihedral angle of 44.5° having D_2 symmetry is also included in Figure 1. In particular a destabilization has occurred for the metal d_{yz} orbital (symmetry b_3) with respect to the tetrahedral system. This orbital is strongly mixed with a π^* orbital (symmetry b_3) of the ligands. In the electronic absorption spectrum the $b_3(d_{yz} + \pi^*) \rightarrow b_3(\pi^* - d_{yz})$ MLCT transition will not be observed since it is symmetry forbidden. This is also the case for the MLCT transition between the lower lying metal d_{xz} orbital (symmetry b_2) and the second π^* orbital of the α-diimine ligands (symmetry b_2). On the other hand, both the $b_3(d_{yz} + \pi^*) \rightarrow b_2(\pi^* - d_{xz})$ and the $b_2(d_{xz} + \pi^*) \rightarrow b_3(\pi^* - d_{yz})$ transitions will be rather intense since they are both z-polarized and since the orbitals involved overlap at this dihedral angle of 44.5°. The two separate bands in the absorption spectrum of $Ni(2,6\text{-}Me_2Ph\text{-}DAB)_2$ are therefore assigned to these MLCT transitions.

(ii) $Ni(CO)_2(\alpha$-diimine). For the $Ni(CO)_2(\alpha$-diimine) complexes one intense absorption band is observed (see Table III) which shows the characteristic solvent dependence of an MLCT transition.[33] The He I and He II photoelectron spectra of $Ni(CO)_2$(tBu-DAB), reported by Andrëa,[51] showed a splitting of the metal d orbitals into two bands (ionization energies of 6.84 and 7.65 eV, respectively) with an intensity ratio of 3/2. This points to a tetrahedral configuration of the metal d orbitals in this complex. Furthermore, two crystal structures of $Ni(CO)_2(\alpha$-diimine) complexes have been published,[41,42] both showing a tetrahedral C_{2v} symmetry. With the use of bond distances and angles of these structures MO CNDO/s calculations have been performed, resulting in an MO diagram for tetrahedral $Ni(CO)_2$(R-DAB) complexes, the relevant part of which is shown in Figure 2A.

(52) Dinjus, E.; Walther, D.; Kaiser, J.; Sieler, J.; Thanh, N. N. *J. Organomet. Chem.* **1982**, *236*, 123.
(53) Bruder, H. Thesis, University of Frankfurt/Main, 1977.
(54) Orgel, L. E. *J. Chem. Soc.* **1961**, 3683.

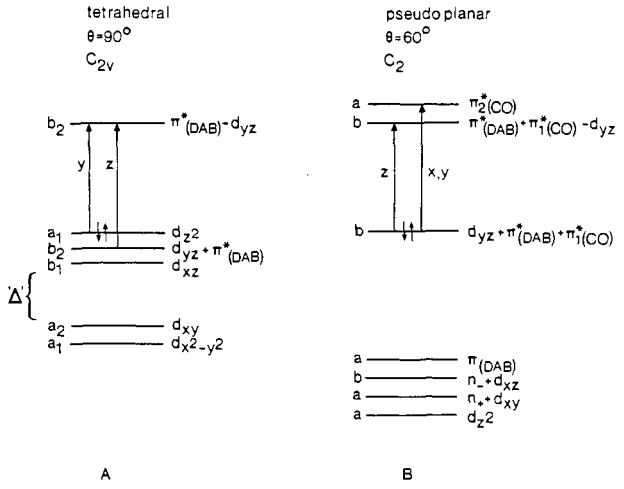

Figure 2. Relevant parts of the MO diagrams, including the electronic transitions with their polarization directions, of $Ni(CO)_2$(R-DAB) complexes with tetrahedral (A) and pseudoplanar (B) structures, assuming a dihedral angle of 60° for the latter compounds.

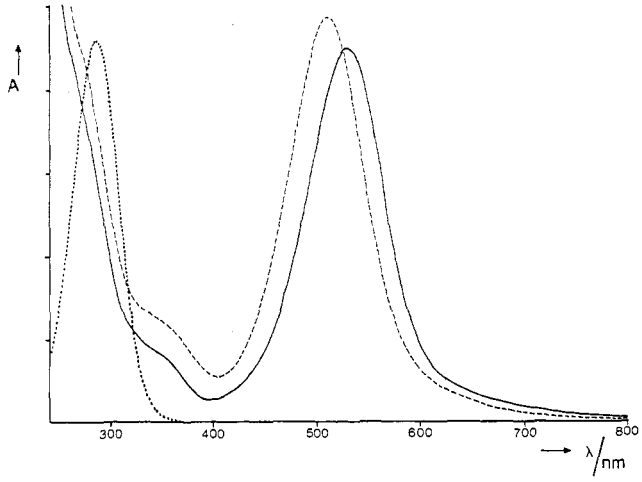

Figure 3. Electronic absorption spectra of $Ni(CO)_2$(tBu-DAB) at 293 K in C_6H_6 (—) and in CH_2Cl_2 (---) and of tBu-DAB in C_6H_6 (···).

Three MLCT transitions are expected from the upper set of the filled metal d orbitals to the lowest empty π^* orbital of the DAB ligand. Only the transitions $a_1(d_{z^2}) \rightarrow b_2(\pi^*_{DAB} - d_{yz})$ and $b_2(d_{yz} + \pi^*_{DAB}) \rightarrow b_2(\pi^*_{DAB} - d_{yz})$ are symmetry allowed (y and z polarized, respectively), the latter being the most intense as a consequence of both the strong overlap between the metal d_{yz} and the ligand π^* orbitals involved and the direction of charge transer parallel to the induced dipole moment along the z axis of the molecule. For $Ni(CO)_2$(tBu-DAB) the large solvatochromism of this band (see Table III) indicates a rather small mixing between these orbitals in this complex.

Figure 3 shows the electronic absorption spectra of $Ni(CO)_2$(tBu-DAB) in two solvents, displaying the characteristic solvent dependence of the main MLCT transition.

The higher energy parts of the spectra in Figure 3 exhibit shoulders at 280 and 350 nm, which are both hardly solvent dependent. The shoulder at 280 nm is assigned to an intraligand (IL) transition found at 285 nm for the free tBu-DAB ligand (also included in Figure 3). The other weaker band at 350 nm is assigned to MLCT transitions from the lower set of metal d orbitals (d_{xy} and $d_{x^2-y^2}$) to the $\pi^*_{DAB} - d_{yz}$ orbital (x and y polarized, respectively). The energy separation between the two MLCT bands in Figure 3 is ca. 8000 cm^{-1}, which is comparable with the splitting of the metal d orbitals observed in the photoelectron spectra of this complex (vide supra).[51]

All other $Ni(CO)_2$(α-diimine) complexes under study show a similar intense MLCT absorption band in the visible region, the position of which depends on the α-diimine ligand, as can be seen from Table III. The solvatochromism of this band, also included in Table III, shows similar trends as were found for the corresponding $M(CO)_4$(α-diimine) (M = Cr, Mo, W) complexes.[20]

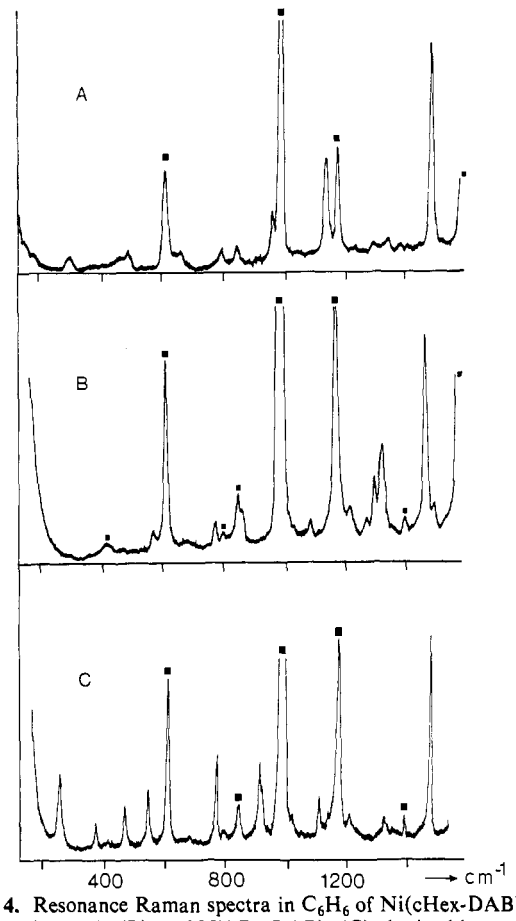

Figure 4. Resonance Raman spectra in C_6H_6 of Ni(cHex-DAB)$_2$ (A), Ni(4-MePh-DAB)$_2$ (B), and Ni(tBu-DAB)$_2$ (C) obtained by excitation at 514.5 nm (■ = solvent band).

The RR spectra, however, clearly show that in particular for $Ni(CO)_2$(2,6-iPr_2Ph-DAB) the character of the main electronic transition differs appreciably from that of the other $Ni(CO)_2$-(α-diimine) complexes because of a difference in structure.

Resonance Raman Spectra. In recent years we have studied in detail the RR spectra of a series of α-diimine complexes in order to characterize their lowest energy MLCT transitions. The RR spectra of the complexes $M(CO)_4$(α-diimine) (M = Cr, Mo, W)[20,33] showed high RR intensities for either metal–ligand or ligand vibrations such as ν_s(CN). These features could be related to the amount of charge transferred during the MLCT transitions just as the solvatochromism of these bands. For the $Fe(CO)_3$-(R-DAB) complexes, on the other hand, only very weak RR effects were observed, mainly for deformation modes of the Fe(R-DAB) metallacycle.[34] From this it was concluded that these complexes after excitation relax to a distorted configuration inducing changes in the bond angles rather than in the bond lengths. In both types of complexes mentioned above, excitation took place into strongly allowed electronic transitions, resulting in A-term or Franck–Condon emission[57] so that only symmetric vibrations were observed in the RR spectra. This is also the case for the Ni–α-diimine complexes. Solutions with optical densities of about 5 were used in order to obtain satisfying spectra with relatively high RR intensities. These RR spectra will now be discussed in detail, starting with the $Ni(R\text{-}DAB)_2$ complexes.

(i) Ni(R-DAB)$_2$. RR spectra of several $Ni(R\text{-}DAB)_2$ complexes have been recorded in order to get more information about the MLCT character of the electronic transitions in connection with the structural differences between these complexes.

Figure 4 shows the RR spectra of three tetrahedral Ni(R-DAB)$_2$ complexes, and the wavenumbers of the resonance-enhanced vibrations together with their assignments are presented in Table IV.

Table IV. Resonance-Enhanced Modes of Ni(R-DAB)$_2$ Complexes[a]

	Raman wavenumbers, cm^{-1}			
vib mode	R = cHex	R = 4-MePh	R = tBu	R = 2,6-Me$_2$Ph[b]
ν_s(NiN)	282 w	*c*	237 m	235 s
δ(NiNCCN)	482 w	560 w	354 w	366 m
	657 w	785 w	461 m	519 w
			539 m	575 m
			775 m	716 s
			916 m	866 s
ν_s(CC)	1141 s	1127 w	1123 m	1210 m
ν(ring)	...	1265 m	...	*c*
		1332 m		
ν_s(CN)	1490 s	1487 s	1502 s	1485 w

[a] Measured in benzene; w = weak, m = medium, s = strong. [b] Excited in the highest energy MLCT band (see Figure 5B). [c] Not observed.

For Ni(cHex-DAB)$_2$ (Figure 4A) strong RR enhancements are observed for the ligand stretching modes ν_s(CN) and ν_s(CC), which characterizes the e($d_{xz} + d_{yz} + \psi^*$) → e($\psi^* - d_{xz} - d_{yz}$) transition in this complex as a transition with considerable MLCT character. Similar features were reported by Leupin et al.[55] for the isoelectronic [Cu(tBu-DAB)$_2$]ClO$_4$ complex, for which a tetrahedral structure was also adopted.[56] Large RR intensities are also found for the ligand modes of Ni(4-MePh-DAB)$_2$ (see Figure 4B). This means that electronic effects have only a small influence on the character of the electronic transitions of these tetrahedral complexes.

Figure 4C shows the RR spectrum of Ni(tBu-DAB)$_2$, which, compared to the spectra of the other tetrahedral Ni(R-DAB)$_2$ complexes, has a somewhat different pattern of resonance-enhanced vibrations. Apart from a strong RR effect for ν_s(CN) RR effects are also observed for ν_s(NiN) and for several deformation modes of the NiNCCN moiety. Ni(tBu-DAB)$_2$ has weaker metal–ligand bonds than Ni(cHex-DAB)$_2$ since its frequency of ν_s(NiN) is much lower (237 cm^{-1} compared with 282 cm^{-1}). This is caused by the bulkiness of the tBu groups.

For all tetrahedral Ni(R-DAB)$_2$ complexes under study no changes in the relative intensities of the RR bands are observed upon excitation at different wavelengths into the MLCT band. This means that the absorption band mainly consists of the strongly allowed *z*-polarized e($d_{xz} + d_{yz} + \psi^*$) → e($\psi^* - d_{xz} - d_{yz}$) transition leading to an excited state with B_2 symmetry (see also Figure 1).

The RR spectra of the pseudoplanar complex Ni(2,6-Me$_2$Ph-DAB)$_2$ obtained by excitation into the two distinct absorption bands of this complex in the visible region are shown in Figure 5. These spectra differ appreciably from those of the tetrahedral Ni(R-DAB)$_2$ complexes shown in Figure 4. Figure 5 shows high RR intensities for ν_s(NiN) and for several deformation modes, whereas hardly any RR effect is observed for the ligand stretching modes. These features are characteristic of transitions between strongly mixed metal d and ligand π^* orbitals. The RR spectrum obtained by excitation into the lowest energy absorption band shows that this band belongs to a transition without any MLCT character (Figure 5A). When the qualitative MO diagram of this pseudoplanar complex (Figure 1B) is taken into account, the lowest energy transition will be the *z*-polarized b_3 ($d_{yz} + \pi^*$) → b_2($\pi^* - d_{xz}$) transition, since in D_2 symmetry transitions between orbitals with equal symmetries are forbidden. As a result of the typical dihedral angle of 44.5° in Ni(2,6-Me$_2$Ph-DAB)$_2$ these $d_{yz} + \pi^*$ and $\pi^* - d_{xz}$ orbitals will overlap, which explains the high intensity of the lowest energy absorption band. It should be noticed in Figure 5A that during this transition in particular metal–ligand bonds are affected.

Figure 5B shows the RR spectrum of this complex upon excitation into the high-energy absorption band. Apart from a weak RR effect for ν_s(CN) this spectrum does not differ much from that of Figure 5A. We therefore assign this higher energy band to the b_2($d_{xz} + \pi^*$) → b_3($\pi^* - d_{yz}$) transition in accordance with the MO diagram of Figure 1B. As expected, this transition has little MLCT character and the strong mixing between metal d and ligand π^* orbitals still dominates the RR spectrum.

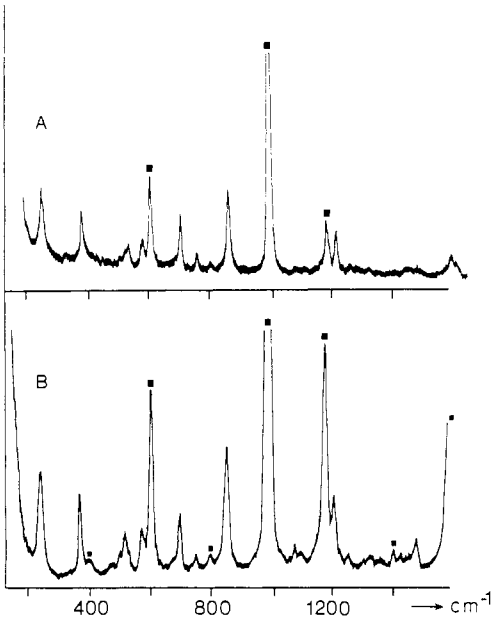

Figure 5. Resonance Raman spectra in C_6H_6 of Ni(2,6-Me$_2$Ph-DAB)$_2$ obtained by excitation at 660 nm (A) and 514.5 nm (B) (■ = solvent band).

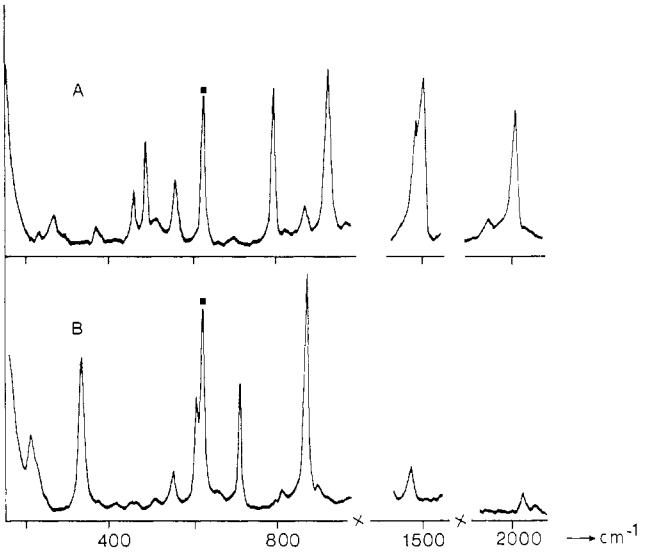

Figure 6. Resonance Raman spectra in C_6H_6 of Ni(CO)$_2$(tBu-DAB) (A) and Ni(CO)$_2$(2,6-iPr$_2$Ph-DAB) (B) obtained by excitation at 514.5 and 540 nm, respectively (■ = solvent band).

Summarizing the RR results of the Ni(R-DAB)$_2$ complexes discussed above, we can say that the structural differences among these complexes also strongly influence their RR spectra. The destabilization of the d_{yz} orbital resulting from the pseudoplanar conformation, as evidenced by MO calculations, explains the occurrence of the absorption band in the 700–800-nm region. Excitation into this band only gives rise to strong RR effects for the metal–ligand modes, in particular for ν_s(NiN), thereby reflecting the strong mixing between metal and ligand orbitals in this complex.

(ii) Ni(CO)$_2$(R-DAB). The relevant parts of the RR spectra of both Ni(CO)$_2$(R-DAB) complexes under study are shown in Figure 6. These spectra exhibit striking differences that at first sight indicate a change of MLCT character of the main electronic transition.

(55) Leupin, P.; Schläpfer, C. W. *J. Chem. Soc., Dalton Trans.* **1983**, 1635.
(56) Daul, C.; Schläpfer, C. W.; Goursot, A.; Pênigault, E. *Chem. Phys. Lett.* **1981**, *78*, 304.
(57) Clark, R. J. H.; Stewart, B. *Struct. Bonding (Berlin)* **1979**, *36*, 1.

The RR spectrum of $Ni(CO)_2$(tBu-DAB) shows relatively large RR intensities for ν_s(CN) at 1500 cm^{-1} and ν_s(CO) at 2006 cm^{-1}. This is in accordance with a transition having considerable MLCT character. Such a RR effect for a carbonyl stretching mode was also reported for the complexes $M(CO)_4$(R-DAB) (M = Cr, Mo, W)[20] and was then explained by a through-space overlap between α-diimine and carbonyl π* orbitals. Strong RR effects are also observed for vibrations at 773 and 913 cm^{-1} belonging to deformation modes of the NiNCCN moiety. The appearance of these bands together with some δ(MCO) modes in the 400–600-cm^{-1} region indicates that $Ni(CO)_2$(tBu-DAB) has a somewhat distorted configuration in the excited state. On the other hand, the metal–ligand bonds are not strongly affected by this MLCT transition. The character of this transition as derived from the RR spectra is therefore in good agreement with that of the *z*-polarized $b_2(d_{yz} + \pi^*_{DAB}) \rightarrow b_2(\pi^*_{DAB} - d_{yz})$ transition of Figure 2A. The second *y*-polarized $a_1(d_{z^2}) \rightarrow b_2(\pi^*_{DAB} - d_{yz})$ transition is too weak to be measured accurately, and in accordance with this, excitation at different wavelengths hardly changed the RR spectrum of $Ni(CO)_2$(tBu-DAB). The spectrum in Figure 6A closely corresponds to that of Ni(tBu-DAB)$_2$ (Figure 4C), in particular with respect to relatively high RR intensities of the deformation modes of the Ni–tBu-DAB metallacycle.

The RR spectrum of $Ni(CO)_2$(2,6-iPr_2Ph-DAB) differs appreciably from that of $Ni(CO)_2$(tBu-DAB) (see Figure 6). In particular two modes in the metal–ligand stretching frequency region show strong RR effects, a band at 209 cm^{-1} belonging to ν_s(NiN) and one at 321 cm^{-1} belonging to ν_s(NiC). These frequencies are clearly lower than those of the corresponding metal–ligand vibrations of $Ni(CO)_2$(tBu-DAB) (vide supra).

The rather low frequency of ν_s(NiC) can be rationalized by taking into account the Ni–C distances and frequencies of several other Ni–carbonyl complexes. A Ni–C distance of 1.763 Å was found for $Ni(CO)_2(PPh_3)_2$,[58] and from a Raman study of other $Ni(CO)_2(PR_3)_2$ complexes it followed that ν_s(NiC) is situated in these complexes at 423–463 cm^{-1}.[59] A longer Ni–C distance of 1.84 Å was reported for $Ni(CO)_4$[60] with a concomitant lower frequency for ν_s(NiC) in the IR spectrum of 371 cm^{-1}.[61] The crystal structure of $Ni(CO)_2$(NMe$_2$-DAB{Me,Me})[37] shows an even longer Ni–C distance of 1.86 (6) Å,[41] revealing the high π-acceptor properties of these DAB ligands. The small value of 321 cm^{-1} for ν_s(NiC) found in the RR spectrum of $Ni(CO)_2$(2,6-iPr_2Ph-DAB) is therefore understandable and will be further corroborated by the structural properties of this complex discussed below. Unfortunately, attempts to prepare the corresponding $Ni(^{13}CO)_2$(2,6-iPr_2Ph-DAB) complex failed since the ^{13}CO pressure obtained from the cylinder was too low.

Apart from high RR intensities for ν_s(NiN) and ν_s(NiC) strong RR effects are also observed for deformation modes of the NiNCCN moiety at 698 and 853 cm^{-1}. The ligand modes ν_s(CN) at 1475 cm^{-1} and ν_s(CO) at 2024 cm^{-1} show only weak RR effects, which means that the electronic transition involved has no MLCT character but is instead strongly metal (d_π)–ligand (π*) bonding to antibonding. This is in accordance with the small solvatochromism of the absorption band of this complex (Table III).

Thus, according to the above RR data the character of the main electronic transition in the visible region changes appreciably upon going from $Ni(CO)_2$(tBu-DAB) to $Ni(CO)_2$(2,6-iPr_2Ph-DAB). We recall here our earlier observations that in the case of Ni(R-DAB)$_2$ this change of character is not in the first place caused by the different electronic properties of the substituents R but rather by their steric requirements, giving rise to a different conformation of the complex. In view of the close correspondence between the RR spectra of the tetrahedral complexes $Ni(CO)_2$(tBu-DAB) and Ni(tBu-DAB)$_2$ on one side and those of the complexes $Ni(CO)_2$(2,6-iPr_2Ph-DAB) and Ni(2,6-Me_2Ph-DAB)$_2$ on the other, a similar deviation from the tetrahedral structure is postulated for the complex $Ni(CO)_2$(2,6-iPr_2Ph-DAB). Unfortunately, this conclusion could not be verified by an X-ray structure determination since no single crystals of this complex could be obtained.

Table V. ^{1}H NMR Data for Ni–R-DAB Complexes

R	δ_R	$\delta_{imine\ H}$	$\Delta_{imine\ H}$[c]
	Ni(R-DAB)$_2$[a]		
cHex	3.0–2.4 and 1.9–1.0 (m, 44 H)	8.86 (s, 4 H)	0.84
tBu	1.94 (s, 36 H)	9.03 (s, 4 H)	1.00
4-MePh	9.04 (d, 8 H); 6.71 (d, 8 H); 1.31 (s, 12 H)	9.82 (s, 4 H)	1.40
2,6-Me_2Ph	7.16–6.80 (m, 12 H); 2.25 (s, 24 H)	7.39 (s, 4 H)	0.07
	$Ni(CO)_2$(R-DAB)[b]		
tBu	1.50 (s, 18 H)	8.07 (s, 2 H)	0.29
2,6-iPr_2Ph	7.27 (m, 6 H); 2.77 (m, 2 H); 1.22 (d, 12 H) 1.10 (d, 12 H)	8.10 (s, 2 H)	0.05

[a] Values (ppm relative to TMS) obtained in benzene-d_6. [b] Values obtained in dichloromethane-d_2 at 213 K. [c] $\Delta_{imine\ H} = \delta_{imine\ H}$(complex) $- \delta_{imine\ H}$(free ligand).

An MO scheme of $Ni(CO)_2$(2,6-iPr_2Ph-DAB), taking into account such a distortion to a pseudoplanar conformation of C_2 symmetry, is presented in Figure 2B. A remarkable feature of this diagram is the mixing in of π*(CO) in both the HOMO and LUMO of this complex. As a result the strongly allowed *z*-polarized $b(d_{yz} + \pi^*_{DAB} + \pi_1{}^*_{CO}) \rightarrow b(\pi^*_{DAB} + \pi_1{}^*_{CO} - d_{yz})$ transition will not only weaken the Ni–N bonds but also the Ni–C bonds. This effect is reflected in high RR intensities for both ν_s(NiN) and ν_s(NiC) (see Figure 6B). However, not only in the lowest excited state but also in the ground state this C_2 complex will have rather weak metal–ligand bonds since the d_{yz} orbital is σ antibonding between the metal and both the R-DAB and CO ligands. This explains the lower frequencies of ν_s(NiN) and ν_s(NiC) observed in the RR spectra of $Ni(CO)_2$(2,6-iPr_2Ph-DAB) compared with those of the tetrahedral $Ni(CO)_2$(tBu-DAB) complex (see Figure 6).

With the use of CPK molecular models it can be demonstrated that the bulky tBu groups in $Ni(CO)_2$(tBu-DAB) prohibit a quasi-planar conformation in this complex. On the other hand, these models clearly show that for $Ni(CO)_2$(2,6-iPr_2Ph-DAB) both tetrahedral and quasi-planar geometries are possible. Our results indicate that the latter conformation is preferred for this complex.

(iii) $Ni(CO)_2$(R-pyca). The RR spectra of both $Ni(CO)_2$(R-pyca) (R = tBu, 2,6-iPr_2Ph) complexes show strong RR effects for ν(CN), ν(py(II)), ν(py(III)) and ν_s(CO). This is in accordance with an *x,y*-polarized $a''(d_{xz},d_{yz}) \rightarrow a''(\pi^*)$ transition within these complexes.[62] These results do not point to structural differences between these complexes as in the case of $Ni(CO)_2$(R-DAB) probably because of the planar pyridine rings of the R-pyca ligands.

^{1}H NMR Spectra. According to tom Dieck and co-workers the structural changes of the Ni(R-DAB)$_2$ complexes are accompanied by changes in the ^{1}H NMR spectra.[46,47] In particular effects on the signals of the imine protons were noticed. These signals shifted downfield with respect to those of the free ligands, but in the case of the pseudoplanar complexes these shifts were very small. We measured the ^{1}H NMR spectra of the Ni–R-DAB complexes under study, and the results are shown in Table V.

It is seen from this table that for the $Ni(CO)_2$(R-DAB) complexes effects similar to those reported by tom Dieck are observed, the pseudoplanar $Ni(CO)_2$(2,6-iPr_2Ph-DAB) thereby showing a very small $\Delta_{imine\ H}$ value of 0.05 ppm compared with 0.29 ppm found for the quasi-tetrahedral $Ni(CO)_2$(tBu-DAB). Although the origin of this effect is not yet fully understood, it is undoubtedly related to the geometry of these complexes.

(58) Krüger, C.; Tsay, Y. H., *Cryst. Struct. Commun.* **1974**, *3*, 455.
(59) Bouquet, G.; Loutellier, A.; Bigorgne, M. *J. Mol. Struct.* **1967**, *1*, 211.
(60) Hedberg, L.; Iijima, T.; Hedberg, K. *J. Chem. Phys.* **1979**, *70*, 3224.
(61) Cârsky, P.; Dedieu, A. *Chem. Phys.* **1986**, *103*, 265.
(62) Cartesian axes for C_s symmetry are used from: Cotton, F. A. *Chemical Applications of Group Theory*; Wiley-Interscience: New York, 1963.
(63) Throughout the text this notation is used to indicate all degrees of mixing between metal and ligand orbitals.

Conclusion

This study clearly reveals structural differences accompanied by characteristic RR properties both for $Ni(R\text{-}DAB)_2$ complexes, for which structural differences have been reported, and for the previously unreported $Ni(CO)_2(R\text{-}DAB)$ complexes. A new application of the RR technique is hereby introduced, demonstrating again the usefulness of this technique for the characterization of allowed electronic transitions of transition-metal complexes. These results will be used to interpret differences in photochemical reactions between $Ni(CO)_2(R\text{-}DAB)$ complexes.[1]

Acknowledgment. We wish to thank Dr. M. W. Kokkes for performing the first experiments leading to this study and Th. L. Snoeck and W. G. J. de Lange for their helpful assistance during the RR experiments and the preparations, respectively. The Netherlands Foundation for Chemical Research (SON) and the Netherlands Organization for the Advancement of Pure Research (NWO) are thanked for financial support.

Registry No. $Ni(CO)_2$(tBu-DAB), 98756-63-9; $Ni(CO)_2$(cHex-DAB), 119679-76-4; $Ni(CO)_2$(iPr-DAB), 119679-77-5; $Ni(CO)_2$(4-MePh-DAB), 119679-78-6; $Ni(CO)_2$(2,6-Me_2Ph-DAB), 119679-79-7; $Ni(CO)_2$(2,6-iPr_2Ph-DAB), 116917-18-1; $Ni(CO)_2$(2,4,6-Me_3Ph-DAB), 119679-80-0; $Ni(CO)_2$(tBu-pyca), 119679-81-1; $Ni(CO)_2$(2,6-iPr_2Ph-pyca), 119679-82-2; Ni(tBu-DAB)$_2$, 63576-87-4; Ni(cHex-DAB), 63576-86-3; Ni(4-MePh-DAB)$_2$, 55926-98-2; Ni(2,6-Me_2Ph-DAB)$_2$, 78802-16-1.

Contribution from the Anorganisch Chemisch Laboratorium, J. H. van't Hoff Instituut, Universiteit van Amsterdam, Nieuwe Achtergracht 166, 1018 WV Amsterdam, The Netherlands

Spectroscopy and Photochemistry of Nickel(0)-α-Diimine Complexes. 2.[1] MLCT Photochemistry of $Ni(CO)_2(R\text{-}DAB)$ (R = tBu, 2,6-iPr_2Ph): Evidence for Two Different Photoprocesses

Peter C. Servaas, Derk J. Stufkens,* and Ad Oskam

Received May 18, 1988

This article describes the low-temperature photochemistry of the complexes $Ni(CO)_2$(tBu-DAB) (I) and $Ni(CO)_2$(2,6-iPr_2Ph-DAB) (II) in different media, in both the absence and the presence of a substituting ligand. The complexes differ in their molecular structure and in the character of their lowest MLCT transitions. The results of this study show that these differences are also responsible for the different primary photoprocesses taking place upon low-energy excitation. Irradiation into the MLCT bands causes breaking of a metal-nitrogen bond in the case of complex I and loss of CO for complex II.

Introduction

Most mechanistic studies in the field of organometallic photochemistry have been concerned with reactions of transition-metal carbonyls such as the mononuclear complexes $M(CO)_6$ (M = Cr, Mo, W), $Fe(CO)_5$, and their derivatives as well as the binuclear metal-metal-bonded complexes $M_2(CO)_{10}$ (M = Mn, Re), $Cp_2Fe_2(CO)_4$, and $Cp_2M_2(CO)_6$ (M = Mo, W).[2-4] All reactions appeared to occur from reactive ^{3}LF states or from a repulsive $^3\sigma\sigma^*$ state in the case of the binuclear complexes.

Introduction of an α-diimine ligand (e.g. 2,2'-bipyridine) in such a complex gives rise to the appearance of one or more metal to α-diimine (MLCT) transitions at low energy. Irradiation into this band leads to population of a ^{3}MLCT state, which is normally much less reactive than the ^{3}LF and $^3\sigma\sigma^*$ states.[5] For, although charge transfer to the ligand leads to a weakening of the metal to α-diimine covalent bond, the ionic interaction between metal and ligand will be strengthened in the excited state. As a result, many transition-metal complexes with a lowest ^{3}MLCT state are not photoreactive, unless energy can be transferred from such a state to a reactive ^{3}LF or $^3\sigma\sigma^*$ state. Especially the energy transfer to a $^3\sigma\sigma^*$ state can be very effective even at low energy, because of the repulsive character of this state.[3,4] Thus, complexes of the type $XMn(CO)_3(\alpha\text{-diimine})$ [X = $Mn(CO)_5$, $Co(CO)_4$, $SnPh_3$] reacted photochemically with quantum yields as high as 0.5-0.8 mol/einstein even upon irradiation with λ = 600 nm.[6-8]

Only recently has a reaction been observed from a reactive ^{3}MLCT state in the case of the α-diimine complexes $Fe(CO)_3$(R-DAB).[9] Low-temperature irradiation with $\lambda > 500$ nm gave rise to a reaction from the lowest ^{3}MLCT state. A completely different reaction was observed upon irradiation of these complexes with $\lambda \leq 500$ nm. The latter reaction occurred from a ^{3}LF state close in energy to the ^{3}MLCT state.

These results concerning the reactivity of ^{3}MLCT states prompted us to study in more detail the photoreactivity of those α-diimine complexes that have only low-energy ^{3}MLCT states and no disturbing ^{3}LF or $^3\sigma\sigma^*$ states.

In this article we report the photochemistry of the two Ni(0) (d^{10}) complexes $Ni(CO)_2(R\text{-}DAB)$ [R-DAB = 1,4-diaza-1,3-butadiene, RN=CH-CH=NR; R = tertiary butyl (tBu), 2,6-diisopropylphenyl (2,6-iPr_2Ph)], which only have a low-energy ^{3}MLCT state.

Up to now, attention has only been paid to the photochemistry of $Ni(CO)_4$, from which the $Ni(CO)_2(R\text{-}DAB)$ complexes are derived.[10-12] Irradiation of this complex gave rise to loss of CO and the appearance of luminescence. These observations have recently been rationalized in terms of the following three-step mechanism:[13]

$$Ni(CO)_4 \xrightarrow{h\nu} Ni(CO)_4^*$$

$$Ni(CO)_4^* \rightarrow Ni(CO)_3^* + CO$$

$$Ni(CO)_3^* \rightarrow Ni(CO)_3 + h\nu'$$

* To whom correspondence should be addressed.

(1) Part 1: Servaas, P. C.; Stufkens, D. J.; Oskam, A. *Inorg. Chem.*, preceding paper in this issue.
(2) Geoffroy, G. L.; Wrighton, M. S. *Organometallic Photochemistry*; Academic Press: New York, 1979.
(3) Meyer, T. J.; Caspar, J. V. *Chem. Rev.* **1985**, *85*, 187.
(4) Stufkens, D. J. Steric and Electronic Effects on the Photochemical Reactions of Metal-Metal Bonded Carbonyls. In *Stereochemistry of Organometallic and Inorganic Compounds*; Bernal, I., Ed.; Elsevier: New York, 1989; Vol. 3.
(5) Meyer, T. J. *Pure Appl. Chem.* **1986**, *58*, 1193.
(6) Andréa, R. R.; de Lange, W. G. J.; Stufkens, D. J.; Oskam, A. *Inorg. Chem.* **1989**, *28*, 318.
(7) Van der Graaf, T.; Rijkhoff, M. Stufkens, D. J.; Oskam, A. to be submitted for publication.
(8) Van Dijk, H. K.; Stufkens, D. J.; Oskam, A. *Inorg. Chem.* **1989**, *28*, 75.
(9) Van Dijk, H. K.; Stufkens, D. J.; Oskam, A. *J. Am. Chem. Soc.* **1989**, *111*, 541.
(10) Thompson, H. W.; Garratt, A. P. *J. Chem. Soc.* **1934**, 524.
(11) Turner, J. J.; Simpson, M. B.; Poliakoff, M.; Maier, W. B. *J. Am. Chem. Soc.* **1983**, *105*, 3898.
(12) Maier, W. B.; Poliakoff, M.; Simpson, M. B.; Turner, J. J. *J. Mol. Struct.* **1982**, *80*, 83.
(13) Rösch, N.; Jörg, H.; Kotzian, M. *J. Chem. Phys.* **1987**, *86*, 4038.

0020-1669/89/1328-1780$01.50/0